IEEE Access
Multidisciplinary ⋮ Rapid Review ⋮ Open Access Journal

Received August 29, 2019, accepted September 21, 2019, date of publication September 24, 2019, date of current version October 7, 2019.

Digital Object Identifier 10.1109/ACCESS.2019.2943479

Flexural Behavior of Fiber Reinforced Cemented Tailings Backfill Under Three-Point Bending

SHUAI CAO[1,2], GAILI XUE[1,2], AND EROL YILMAZ[3]

[1]State Key Laboratory of High-Efficient Mining and Safety of Metal Mines of Ministry of Education, University of Science and Technology Beijing, Beijing 100083, China
[2]School of Civil and Resources Engineering, University of Science and Technology Beijing, Beijing 100083, China
[3]First Quantum Minerals Ltd., Cayeli Bakir Isletmeleri A.S., TR53200 Rize, Turkey

Corresponding author: Erol Yilmaz (yilmazer@fqml.com)

This work was supported in part by the National Natural Science Foundation of China under Grant 51804017, in part by the China Postdoctoral Science Foundation under Grant 2018M631341, in part by the Open Fund of the Key Laboratory of Ministry of Education for Efficient Mining and Safety of Metal Mines under Grant USTBMSLAB201804, and in part by the Fundamental Research Funds for the Central Universities under Grant FRF-TP-17-075A1.

ABSTRACT Mining methods use cemented tailings backfill (CTB) for filling mined-out voids and make operations safer since employees are working under it. Hence, the durability behavior of CTB is of great importance in applications, for example, in the assessment of slope stability when extracting ore left in neighboring stopes. Addition of cement content would increase the strength of CTB but creates extra costs to mines. To cut cement-related costs as well as improve durability, different types of fibers are added to CTB samples. This paper aims to analyze flexural behavior of fiber reinforced CTB samples under three-point bending loading. To do so, a comprehensive laboratory work was undertaken to explore the effect of fiber reinforcement on bending resistance of CTB samples, based on orthogonal experimental design. The effect of fiber type (FT), fiber content (FC), solid content (SC) and cement-to-tailings ratio (c/t) on bending characteristics was investigated. Results indicate that the addition of fiber enhances the bending strength of fiber reinforced CTB samples and the bearing capacity after the peak in the load-deflection curve. Fibers help correct the faintness of CTB samples by mobilizing tensile strength along the failure planes. The crack resistance of fiber is reflected in the crack propagation stage. Secondly, the order of the sensitivity of four factors on bending strength of fiber reinforced CTB samples is as follows: c/t > SC > FT > FC. Lastly, the main findings of this study can provide a major reference for CTB's last design in underground mining.

INDEX TERMS Cemented tailings backfill, fiber types and properties, bending strength testing, load-deflection analysis, microstructural characteristics.

I. INTRODUCTION

Underground mining is one of the main ways to obtain metal and non-metallic mineral resources. In comparison with surface mining, underground extraction of ores is cost-effective if the excavated orebodies provide relatively high head grades [1]–[3]. There are numerous underground mining methods with and without backfilling, considering the ore being mined and the nature of the orebody [4]–[6]. Likewise, advanced tools and technologies offer more productivity and safer mining in underground operations, leading to a major decrease in the cost of production methods [7]–[10]. The safe, efficient and economical recycling resources have gradually become the primary focus of mining companies worldwide [11]–[14]. For underground mining of metal mines, mining method with the backfill has been commonly used due to its high recovery rate, reliable safety and reduced the surface tailings storage requirement [15]–[18]. Indeed, the safe and efficient mining of soft orebody is a big technical problem that needs to be solved urgently by the most modern mining industries all around the world [19]–[22]. The methods applied for mining such orebodies are overhand cut and fill (OHCF) and underhand cut and fill (UHCF) mining methods [23]–[27]. Compared with sublevel stoping and shrinkage, cut and fill mining offer the advantage of full selectivity and is preferred in situations where orebody dips steeply [28], [29]. In this technique, the voids created by mining is backfilled with an engineered mix of tailings

The associate editor coordinating the review of this manuscript and approving it for publication was Navanietha Krishnaraj Rathinam.

(frequently added cement for obtaining a strong backfill mass), which helps support the walls of underground voids [30]–[33]. This type of mining is often done upwards from lower levels, so the fill is used for ensuring a new working level for further mining [34].

Mines such as Jiaojia Gold Mine and Jinchuan Nickel Mine are typical soft rock mines in China and their mining methods are UHCF [35], [36]. Mining workers and equipment are directly exposed under cemented tailings backfill (CTB; it consists usually of filtered tailings, hydraulic cements and mix water) [37]. When the UHCF mining method is typically used for underground mining, the stability of CTB during mining cycle is vital to ensure the safety of personnel and tools since an unexpected collapse may happen during mining [23]. Besides, collapse and bending deformation are the two main failure modes of CTB [38], [39]. As mines go deeper as a result of the increased demand for metals caused by global economic growth and exploitation of shallow mineral deposits, the stress of surrounding rock increases importantly and hence the encountered ground conditions in excavated stopes become more challenging [4]. To ensure a secure working platform for most mines, UHCF with CTB has become a more widely used mining method [2], [10], [40].

The strength and durability of CTB is a significant issue in UHCF mining method because of miners working under it [29]. Hence, the strength properties of CTB samples should be improved via insertion of mineral and chemical additives, such as binding agents, natural or artificial pozzolans and fibers [21], [28], [32]. The improvement of paste backfill by cement addition increases its stiffness, but increases its brittleness, causing the enhanced mass to fail in a brittle way [41]–[43]. Alternatively, fiber addition enhances the ductility and stability of reinforced CTB without affecting the strength of the created mass [44]–[48]. Addition of randomly oriented fibers to cementitious material creates an engineered mix which has enough strength properties and post-rupture load bearing capacity and offers a relatively low-cost alternative solution in its geotechnical design [49]–[52]. Figure 1 shows a three-point bending mechanical model of overlying CTB in the UHCF mining method. Overall, CTB with the false roof falling off and collapsing to the stope is mostly layered and block shaped. Can the fiber material be ''cracked rather than broken'' under the bending loading? Can we explore the preparation of fiber reinforced CTB with low cost, high overall strength, good flexural and crack resistance, which can reduce the secondary dilution caused by the backfilling of CTB mass into mined-out stope, and can realize safe and efficient recovery? This study clarifies these issues.

Mitchell and Stone [53] firstly proposed the method of fiber reinforcement for the design of mine backfill in order to reduce the overall cement usage. They found that adding fibers could obviously increase the tensile and flexural strength of structures [54]. Researches on the CTB reinforced with fibers have recently become a hot issue for hard

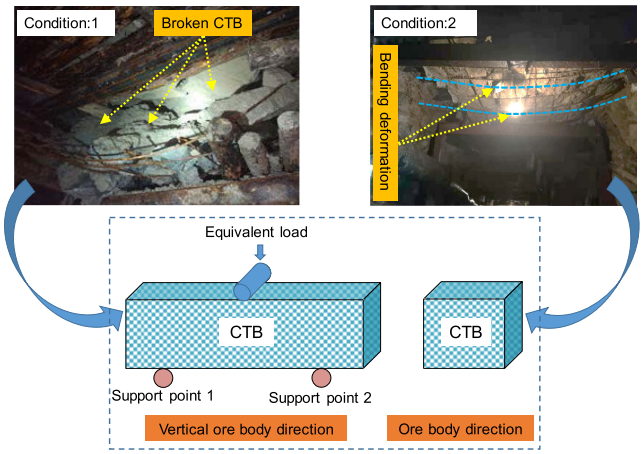

FIGURE 1. Physical model of overlying CTB in UHCF mining method.

rock mines. The research field mainly involves rheology, uniaxial compression, bending test and physical models of fiber reinforced CTB samples [55]–[57].

The techniques used mainly include numerical simulation codes and laboratory tests [58]–[60]. To better study the fiber-reinforced mechanisms of CTB samples, Xue *et al.* [37], [61], [62] done several experiments including uniaxial compressive strength test, Brazilian tensile test and three-point bending test. The researchers found that the fibers made a positive contribution on strength properties of CTB reinforced with different types of fibers. Similar results were also reported [63]–[68]. However, researchers not only focus on strength of fiber reinforced CTB samples, but its rheological properties are also important factors during its industrial applications. Zhang *et al.* [69] found that the apparent viscosities, plastic viscosities and the yield stress of cement paste increase with increasing length and dosage of polypropylene fiber. Galicia-Aldama *et al.* [56] reported that the compressive strength and rheological behavior of the studied material were drastically improved when the coconut fibers were added in different percentages and three aspect ratios.

The originality of this paper consists in the evaluation of the influence of fiber type (FT), fiber content (FC), solid content (SC) and cement-to-tailings ratio (c/t) on flexural behavior of CTB reinforced with diverse types of fibers. A total of four FTs (polypropylene, polyacrylonitrile, glass and polyvinyl alcohol), four FCs (0.2%, 0.4%, 0.6% and 0.8%), four SCs (65%, 68%, 70% and 75%) and four c/ts (1:4, 1:6, 1:8 and 1:10) was selected as main variables. The orthogonal experimental method was used to study bending mechanical properties of fiber reinforced CTB samples. To conclude, the microstructure of CTB samples with fiber was also examined by scanning electron microscopy (SEM) to better reveal the fiber reinforced mechanisms.

II. EXPERIMENTAL PROGRAM

The research conducted in this study was divided in two parts. Part one consisted of depicting the properties of the materials

used during experiments. Part two consisted of explaining the techniques used in the molding process and undertaken laboratory testing.

A. MATERIALS

The materials used in performed experiments were tailings, fibers, cement and water. The detailed characterizations of these materials are presented in the following sub-sections.

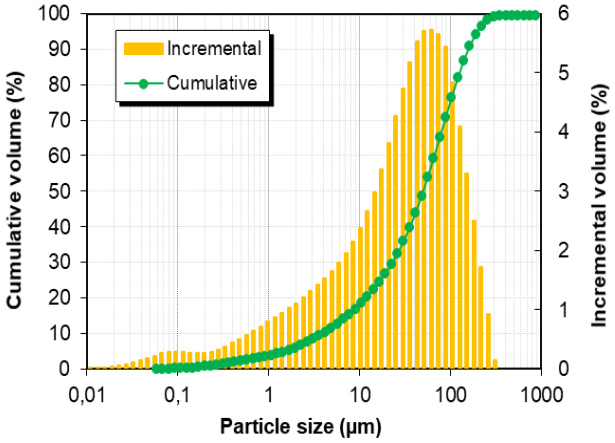

FIGURE 2. Particle size distribution curves of the tested tailings sample.

1) PROCESSING TAILINGS

The tailings sample used in this study was collected from a gold mine located in Shandong, a northern coastal province in Eastern China. FIGURE 2 shows both incremental and cumulative particle size distribution (PSD) curves of the tested tailings sample. The proportion of particles under 20 μm accounted for 27%, which indicates a good ability to retain enough water to form a suitable paste material [70]. According to the gradation theory, the ratio of limiting grain size (d_{60}) to the effective particle size (d_{10}) is referred to as the non-uniformity coefficient (C_u: D_{60}/D_{10}). To prevent discontinuous gradation, C_u of the tailings should be higher than 10 [71]. The coefficient values of uniformity (C_u) and curvature (C_c: $D_{30}^2/D_{60} \times D_{10}$) are 15.63 and 1.84, respectively. The executed chemical analysis has well shown that the total content of SiO_2, Al_2O_3, CaO and MgO main oxides assumed for 82.4% of the studied tailings, which may generate acids and/or leachates.

2) FIBER TYPES AND CHARACTERISTICS

To rise the internal quality, reduce the maintenance cost and prolong the service life of cement mortar, backfill, and concrete, fiber is designed for use in cementitious materials. Fibers can mostly reduce the formation of shrinkage cracking in cement mortar, backfilling and concrete prior to curing process, thereby considering a serious increase both strength and durability of the studied test material [47]. Four different types of fiber (polypropylene, polyacrylonitrile, glass and polyvinyl alcohol) were employed, as shown in FIGURE 3.

FIGURE 3. Four kinds of fibers: (a) polypropylene; (b) polyacrylonitrile; (c) glass; (d) polyvinyl alcohol.

TABLE 1. The basic physical and mechanical properties of fibers used.

Fiber type	Length (mm)	Density (g/cm^3)	Tensile strength (MPa)	Young's modulus (GPa)	Elongation rate (%)
Polypropylene	12	0.91	398	3.85	28.0
Polyacrylonitrile	12	0.91	736	4.68	30.0
Glass	12	2.02	369	4.89	36.5
Polyvinylalcohol	12	1.30	1400	3.80	17.0

The basic physical and mechanical properties of fibers were listed in TABLE 1. The fiber content used in this study is 0.2%, 0.4%, 0.6% and 0.8% by the weight of the sum of dry tailings and cement.

3) BINDER AND WATER

A small dosage (it typically varies from 2 to 9wt%) of hydraulic binder is added to CTB samples for enhancing its mechanical strengths. Most modern mines are now searching for alternative cementitious materials, such as fly ash, silica fume and slag in order to cut their high cement-related costs [72]. In this study, ordinary Portland cement OPC 42.5 was used as the main binding agent. The physical and mechanical properties of the used cement are listed in TABLE 2.

TABLE 2. Chemical component of ordinary Portland cement OPC 42.5.

Varieties, (%)	SiO_2	Fe_2O_3	Al_2O_3	MgO
OPC 42.5	20.37	3.28	4.85	3.61
Varieties, (%)	CaO	SO_3	Specific surface area, (m^2/kg)	
OPC 42.5	63.32	1.72	0.16	

Additionally, the mixing water is crucial for any type of mine backfill since it can cause a strength reduction for a given CTB recipe and curing time. Mix water can be clean water like tap water or contaminated mine water like process water [73]. In this study, tap water as mix water was used to thoroughly mix binder and tailings.

B. METHODOLOGY

1) ORTHOGONAL EXPERIMENTAL DESIGN

The orthogonal table can balance sampling in the range of factors, so that each test has a strong representativeness, and these tests can often achieve the experiment's purpose. As stated by the analysis results of the previous experimental

data, FT, FC, SC and c/t are important factors which greatly affect the strength gaining of fiber reinforced CTB samples. To systematically explore the bending resistance of fiber reinforced CTB samples and reduce experimental workload, the orthogonal experimental design scheme of 4 factors (FT, FC, SC and c/t) and 4 levels is adopted in the present paper. The fundamental design parameters of specific experimental scheme are listed in TABLE 3.

TABLE 3. Orthogonal experimental design parameters.

Factor level	FT	FC (wt.%)	SC (wt. %)	c/t
1	Glass	0.2	65	1:4
2	Polypropylene	0.4	68	1:6
3	Polyacrylonitrile	0.6	70	1:8
4	Polyvinyl alcohol	0.8	75	1:10

2) MOLDING AND CURING OF SPECIMENS

Tailings, fiber, binder and water were mixed for at least 15 min to prepare the rectangular fiber reinforced CTB samples in this experiment. Moreover, the length, width and height of specimens are 160 mm, 40 mm and 40 mm, respectively. The span ratio is 2.5, and the effective span is 100 mm. Fiber reinforced CTB samples were made with various FTs, FCs and SCs. SC was set as 65%, 68%, 70% and 75%. c/t values are 1:4, 1:6, 1:8 and 1:10 respectively. The prepared samples reinforced with different types of fibers were demounted and cured in a relative humidity at 95 ± 5% and temperature at 20 ± 5°C for a curing time of 7 days. All materials for the sample preparation were weighed by electronic scale with an accuracy of 0.01g. FIGURE 4 shows fiber reinforced CTBs used during the experiments.

FIGURE 4. Photos of rectangular fiber reinforced CTB samples.

3) LOAD-BENDING STRENGTH TESTING

Fiber reinforced CTB samples were subjected to flexural tests (by three-point bending) according to ISO 679-2009 and GB/T 50081-2002 standard procedures [74]. A 10kN microcomputer controlled electronic universal testing system in the

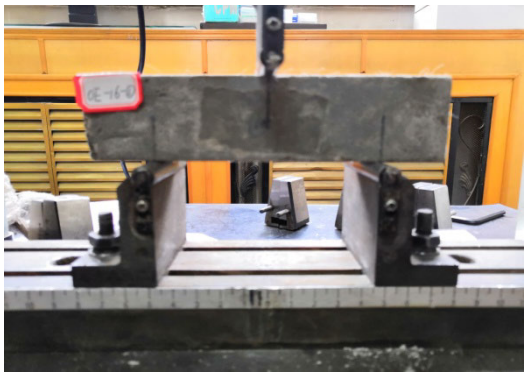

FIGURE 5. Photo of the three-point bending equipment used.

University of Science and Technology Beijing was used for bending loading. All experimental data can be automatically recorded and saved during the three-point bending loading process. All fiber reinforced CTB samples were tested in a strain-control mode at a loading rate of 0.1 mm/min until failure. FIGURE 5 shows a photo of the three-point bending testing system used in this study.

a: BENDING STRENGTH CALCULATION

The bending strength of FRCTB samples were conducted by the three-point bending method. The normal bending stress was calculated as follows:

$$\sigma_1 = \frac{3pL}{2bh^2} \tag{1}$$

where, σ_1 represents the bending strength (kPa), p denotes the maximum breaking load (N), b stands for the specimen width (mm), h refers to the specimen height (mm) and L refers the span length (mm).

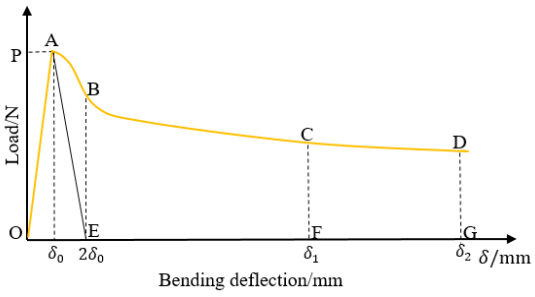

FIGURE 6. Schematic diagram of energy absorption calculation of fiber reinforced CTB beam.

b: EQUIVALENT BENDING STRENGTH

FIGURE 6 show a schematic view of energy absorption calculation of fiber reinforced CTB beam. P is the peak load (N), δ_0 represents the deflection value at the peak load (mm), when the deflection value is $2\delta_0$, the energy absorption value of the initial crack is the area of the triangle OAE (N·mm), δ_1 is the deflection value when the slope of the load deflection curve

is close to zero after the peak load (mm), δ_2 is the deflection value at the end of the fiber action period (mm).

The equivalent bending load (F_1, F_2) and equivalent bending strength (f_1,f_2) for the deflections δ_1 and δ_2 are calculated as follows:

$$Q = \int_0^{\delta} P(\delta) d_{\delta} \tag{2}$$

$$F_1 = \frac{2Q_1}{2\delta_1 - 3\delta_0} \quad F_2 = \frac{2Q_2}{2\delta_2 - 3\delta_0} \tag{3}$$

$$f_1 = \frac{3F_1 L}{2bh^2} \quad f_2 = \frac{3F_2 L}{2bh^2} \tag{4}$$

where, Q_1 and Q_2 are the energy absorption values of the fiber contribution to fiber reinforced CTB beam when the deflection is δ_1 and δ_2, that is, the area of ACFE and ADGE (N · mm). In addition, L, b and h are span, width and height, respectively.

c: SEM OBSERVATIONS

Firstly, some samples were separated from the destroyed fiber reinforced CTBs. The microstructure of CTB with fiber was analyzed using a scanning electron microscopy (SEM) named ZEISS EVO 18, Germany. The main parameters of SEM tool are resolution: 3.0 nm; acceleration voltage: 200V-30kV, 10V step continuously adjustable; image electrical translation: $\pm 50\mu$m; magnification: 5 $\sim$ 1000,000, nonstop adjustable and the vacuum pump system: turbo-molecular plus mechanical pump, no cooling water required. FIGURE 7 shows SEM tool and CTB after vacuum.

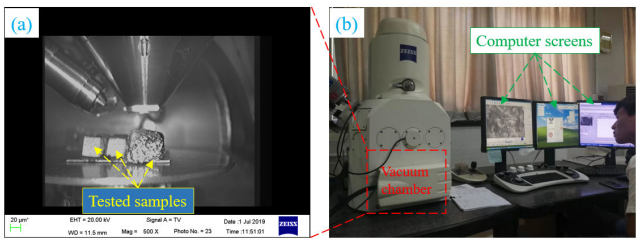

FIGURE 7. SEM test sample (a) and samples prepared after vacuum (b).

III. RESULTS AND DISCUSSION

A. LOADING-DEFLECTION CURVE AND BENDING STRENGTH ANALYSIS

The load-deflection curves of each fiber reinforced CTB in the orthogonal test were plotted, as shown in FIGURE 8. If fibers in the most dangerous surface of CTB are unplugged, they are the end of fiber action. Given that the fiber length used in this test was 12 mm, combined with peak deflection (approximately 0.5 mm) and geometric relationship between the maximum width of the crack and maximum deflection, the final loading displacement was set to 8 mm, that is, the mid-span deflection was 8 mm. FIGURE 8 shows a gradual increase of the mid-span deflection, and the load-deflection curve of each CTB begins to decrease after reaching the peak load. But no rapid decrease was observed for

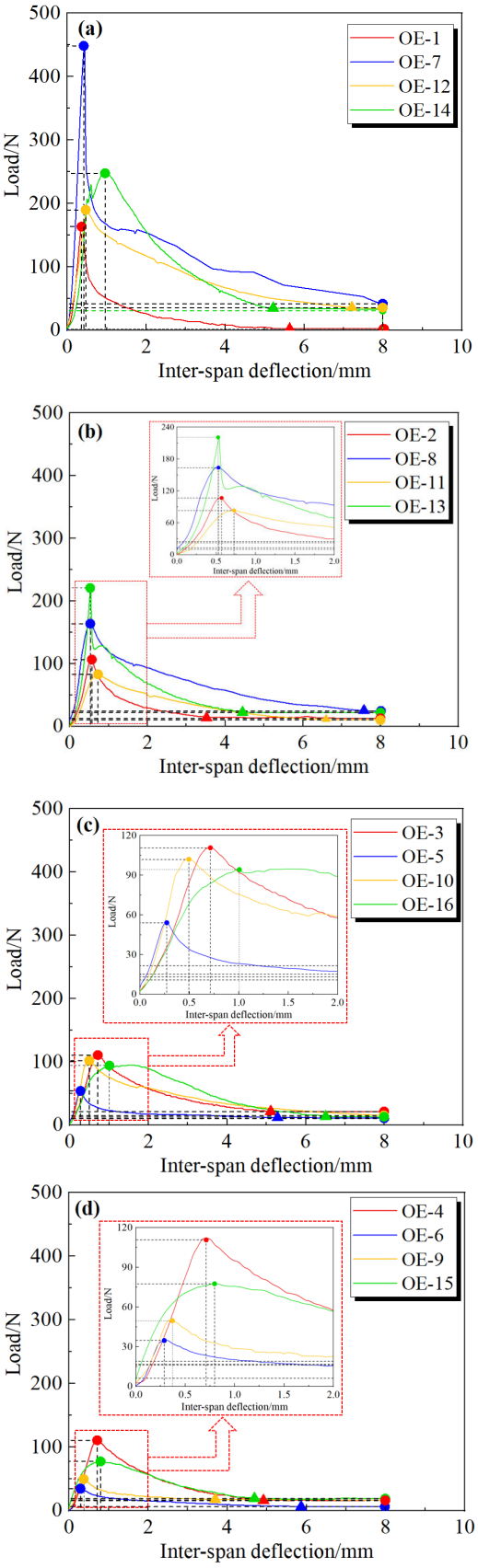

FIGURE 8. The load-deflection curve of fiber reinforced CTB samples: (a) c/t: 1/4, (b) c/t: 1/6, c/t: 1/8 and (d) c/t: 1/10.

the load value after the peak, and the strain softening stage occurs. When the mid-span deflection reached a certain value, the load was almost no longer reduced, but entered a gradual descent phase (the tangent slope is zero) until the end of load phase.

The influence of four factors at four levels on bending strength of fiber reinforced CTB samples was analyzed by range analysis, and their effect on bending strength was plotted in TABLE 4 and FIGURE 9. Test no. OE-1 are denoted as fiber reinforced CTB sample number, where capital "OE" signifies orthogonal experiment (OE), and "1" represents the tested sample number.

TABLE 4. Orthogonal experimental results of the bending strength of fiber reinforced CTB samples.

Test No.	FT	FC (wt.%)	SC (wt.%)	c/t	Bending strength, (kPa)
OE-1	Glass	0.2	65	1:4	508
OE-2		0.4	68	1:6	273
OE-3		0.6	70	1:8	275
OE-4		0.8	75	1:10	239
OE-5	Polypropylene	0.2	68	1:8	144
OE-6		0.4	65	1:10	109
OE-7		0.6	75	1:4	1195
OE-8		0.8	70	1:6	431
OE-9	Polyacrylonitrile	0.2	70	1:10	138
OE-10		0.4	75	1:8	269
OE-11		0.6	65	1:6	236
OE-12		0.8	68	1:4	524
OE-13	Polyvinyl alcohol	0.2	75	1:6	558
OE-14		0.4	70	1:4	642
OE-15		0.6	68	1:10	197
OE-16		0.8	65	1:8	239
K1	1294.7	1347.5	1091.4	2869.5	
K2	1878.4	1293.2	1138.7	1497.5	
K3	1166.3	1902.7	1485.7	926.3	
K4	1636.5	1432.4	2260.1	682.6	
k1	323.7	336.8	272.8	717.4	
k2	469.6	323.3	284.6	374.4	
k3	291.6	475.7	371.4	231.6	
k4	409.1	358.1	565.0	170.7	
R	178.0	152.4	292.1	546.7	

According to TABLE 4 and FIGURE 9, when the bending strength value was higher than 500 kPa, the experimental results numbered OE-1, OE-7, OE-12, OE-13, and OE-14 were in accordance with the requirements.

Four groups obtained a c/t of 1:4, and three groups exhibited a solid content greater than or equal to 70 wt.%. This result shows that the order of the weight of influence of the four factors on the bending strength of fiber reinforced cement-tailings matrix composites is as follows: c/t > SC > FT > FC. The cement-to-tailings ratio and solid content are still two main factors that affect bending strength, while fiber type and content are secondary factors with the effect of the former being higher than that of the latter.

From FIGURE 9, the main conclusions are as follows: (1) Polypropylene fiber has an ideal effect on bending strength of CTB in four different fiber types. The bending strength of CTB with polypropylene fiber was 1.45, 1.61,

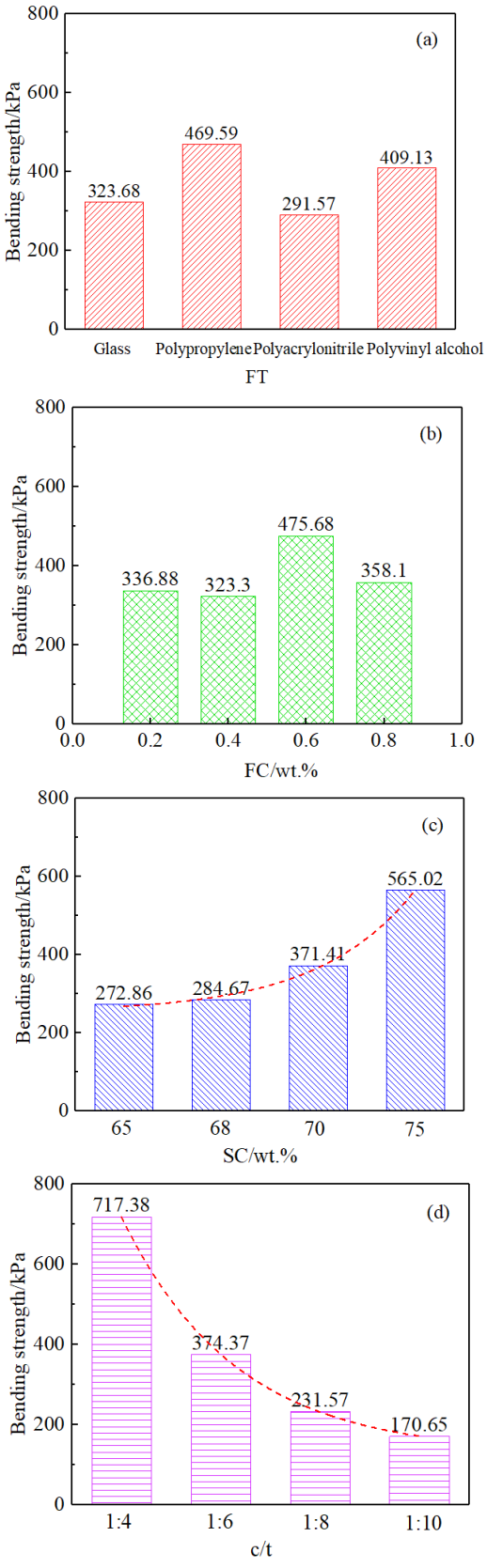

FIGURE 9. Effect of different factors on bending strength of CTB.

and 1.15 times that of glass fiber, polyacrylonitrile fiber, and polyvinyl alcohol fiber CTB. 2) When the fiber content in CTB was 0.6 wt%, the corresponding bending strength was the highest, and its strength value was 475.68 kPa. This is mostly because of a dense microstructure and a well adhesion and interface between fiber and CTB, reducing crack propagation.

(3) With the increase of SC, the bending strength of fiber reinforced CTB increases gradually. Compared with the bending strength of one-level lower concentration sample, the increase rates of specimens with 67 wt.%, 68 wt.%, and 75 wt.% SC were 4.33%, 30.47%, and 52.13%, respectively. (4) With the decrease of c/t, the bending strength of fiber reinforced CTB samples decreases gradually. Compared with the bending strength of the one-level lower lime-sand ratio specimen, the increase rates of the specimens with c/ts of 1:8, 1:6, and 1:4 were 35.7%, 61.67%, and 91.62%, respectively. Thus, the larger the c/t ratio the higher the corresponding increase rate. During the bending test design of CTB sample, the appropriate c/t can be determined first according to bending mechanical strength requirements.

B. EQUIVALENT BENDING STRENGTH

Based on the variation characteristics of load-deflection curve of fiber reinforced CTB samples in FIGURE 9, by using the evaluation method of the fiber concrete standard [75], the equivalent load and the equivalent bending strength were calculated, and then post-peak deformation properties were analyzed. FIGURE 4 shows the effect of bending strength at the level of each factor. According to the calculation results of the energy method, the range of values of δ_1/δ_0 is 5.4 to 21.2, that is, the deflection value of fiber reinforced CTB entering the yield stage is considerably greater than the peak deflection, indicating that CTB can still withstand a large deformation value after the initial crack.

TABLE 5. Equivalent bending strength statistics of fiber reinforced CTB.

Test No.	δ_0/mm	δ_1/mm	δ_2/mm	f_1/kPa	f_2/kPa
OE-1	0.37	5.6	8.0	52	40
OE-2	0.57	3.5	8.0	71	49
OE-3	0.70	5.1	8.0	103	81
OE-4	0.70	4.9	8.0	95	69
OE-5	0.25	5.3	8.0	50	44
OE-6	0.29	5.9	8.0	40	34
OE-7	0.43	8.0	8.0	241	241
OE-8	0.52	7.6	8.0	153	148
OE-9	0.34	3.7	8.0	60	50
OE-10	0.47	8.0	8.0	89	96
OE-11	0.71	6.6	8.0	87	77
OE-12	0.50	7.2	8.0	208	197
OE-13	0.54	4.4	8.0	123	91
OE-14	0.97	5.2	8.0	236	174
OE-15	0.77	4.7	8.0	103	79
OE-16	1.00	6.5	8.0	119	101

TABLE 5 lists the equivalent bending strength statistics of fiber reinforced CTB samples. According to analysis of the effect of equivalent bending strength f_1, the ranges between FT, FC, SC, and c/t are 65 kPa, 72.5 kPa, 63.5 kPa and 109.75 kPa, respectively. The order of influence (from large to small) is c/t, FC, FT, and SC. According to an analysis of the effect of equivalent bending strength f_2, the ranges between FT, FC, SC, and c/t are 57 kPa, 72.5 kPa, 61.5 kPa and 105 kPa, respectively; and the influential effect from high to low is c/t, FC, SC, and FT.

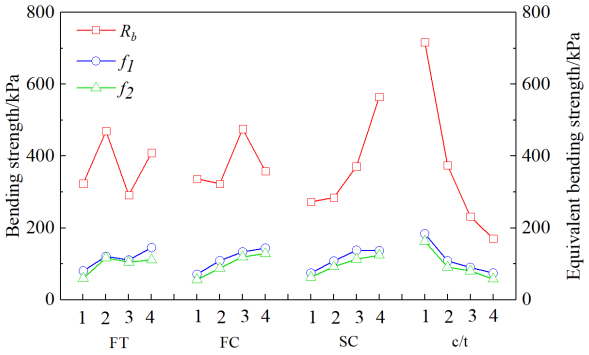

FIGURE 10. Effect of bending strength at various factor levels.

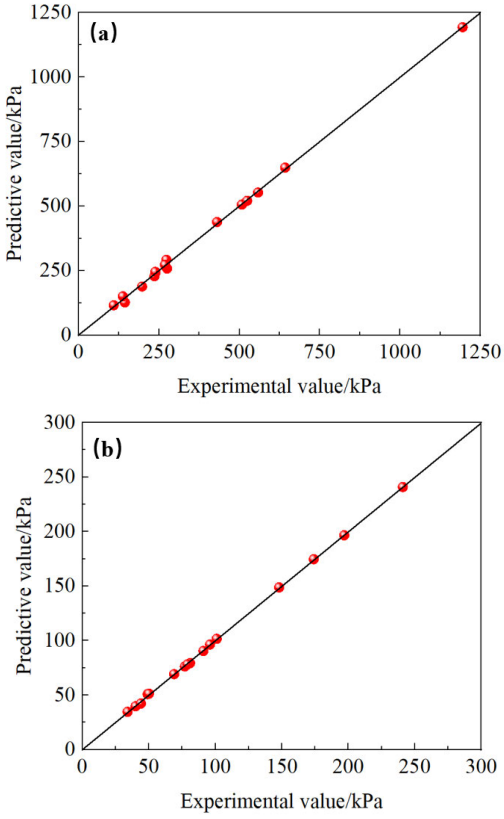

FIGURE 11. Experimental vs. predictive values: (a) bending strength; (b) equivalent bending strength.

In addition to the influential effects of four factors (peak load here), bending strength is mainly affected by c/t and SC; and the equivalent bending strengths f_1 and f_2 after peak is mainly affected by c/t and FC. FIGURE 10 shows the effect of bending strength at various factor levels.

According to FIGURE 10, the following conclusions are obtained: (1) The effect of fiber type on bending strength and

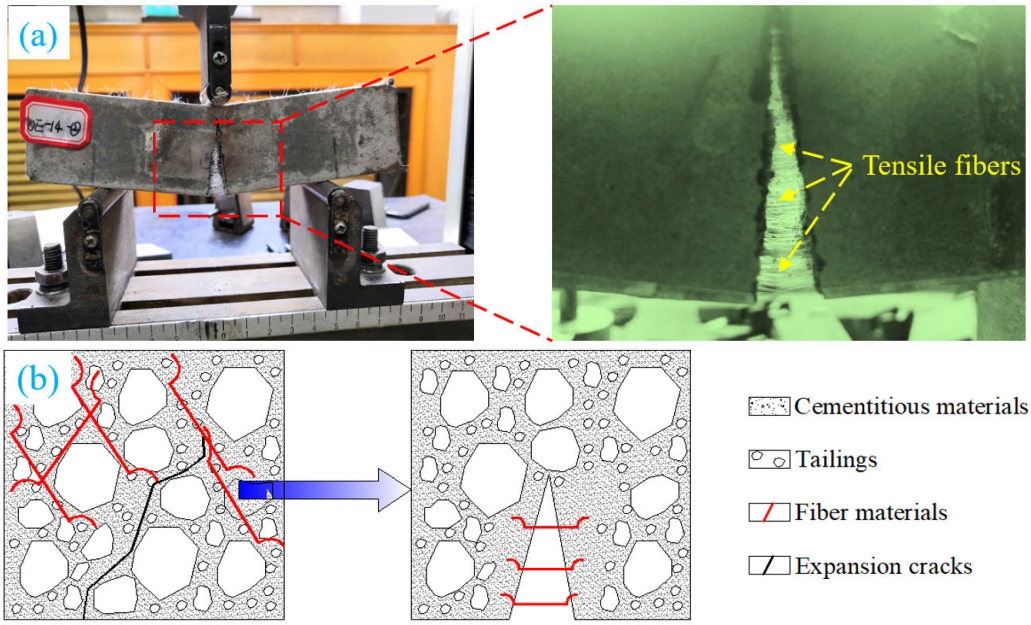

FIGURE 12. Schematic view of fiber-reinforced mechanism on CTB: (a) experimental situation; (b) plot of crack develops in fiber reinforced CTB.

equivalent bending strength of CTB samples was the same and determined by the performance parameters of fiber. The glass fiber has a high modulus of elasticity, that is, it has high rigidity, but has poor alkali resistance, and is affected by corrosion of hydration product, so that glass fiber loses its original characteristics with the extension of curing time.

The polypropylene fiber is easy to disperse, improves the uniformity of CTB, reduces the segregation rate of the filling body, and has good affinity in matrix. The polyacrylonitrile fiber contains a hydrophilic group (-CN) in its molecular structure, so that fiber has good bonding property with the filler. Polyvinyl alcohol fibers have poor adsorption properties to cement particles and poor water retention, making it difficult to exert the desired reinforcing effect. (2) As the fiber dosage increased, the bending strength increased first and then decreased, and the optimum content was 0.6 wt. %; the equivalent bending strength, however, increased gradually. The ratio of equivalent bending strength f_2 to bending strength was 16.7%, 27.3%, 25.12%, and 35.95%, which were obtained at four different content levels. In addition, compared with the equivalent bending strength at the previous level, when the contents were 0.4, 0.6, and 0.8 wt.%, the increase rates of f_1 were 52.9%, 22.5%, and 7.7%, respectively; and the increase rates of f_2 were 56.9%, 35.4%, and 7.7%, respectively. (3) With the increase of SC, the bending strength and equal bending strength increased gradually. When SC were 68, 70, and 75 wt.%, the increase rates of f_1 were 44.9%, 27.8%, and -0.7%, respectively; and the increase rates of f_2 were 46.43%, 22.76%, and 9.71%, respectively. Hence, increasing the fiber content and SC increased the bending resistance of CTB after the peak, but the improvement effect decreased gradually. (4) With the decrease of c/t, the bending strength and equivalent bending strength decreased gradually. The ratios of f_2 to bending strength under four different c/t conditions were 22.72%, 24.37%, 34.76%, and 33.99%. The larger the c/t, the higher the brittleness of fiber reinforced CTB and the greater the decrease of the bending performance after the peak.

C. ESTABLISHMENT AND VERIFICATION OF BENDING STRENGTH PREDICTION MODEL

The quadratic polynomial regression analysis method is based on orthogonal design scheme and uses the regression analysis method to derive the mathematical relationship model between the given multiple independent variables and dependent variables. Thus, in combination with the above test results, the regression equations for bending strength σ_1 and equivalent bending strength f_2 are derived:

$$\begin{aligned}\sigma_1 = {} & -354.076 + 729.335x_1 + 5010.151x_2 + 93.379x_3 \\ & - 33196.447x_4 - 20.38x_1^2 \\ & + 235.908x_2^2 - 911.233x_3^2 + 15961.308x_4^2 \\ & - 188.355x_1x_2 - 622.81x_1x_3 - 889.306x_1x_4 \\ & - 5830.845x_2x_3 - 4293.15x_2x_4 + 51708.388x_3x_4 \\ f_2 = {} & -6059.642 + 105.623x_1 + 1646.746x_2 + 16515.74x_3 \\ & - 5992.007x_4 - 19.126x_1^2 \\ & + 21.295x_2^2 - 11314.738x_3^2 + 5038.131x_4^2 \\ & + 23.302x_1x_2 - 40.156x_1x_3 + 45.857x_1x_4 \\ & - 2069.649x_2x_3 - 1101.712x_2x_4 + 7662.766x_3x_4\end{aligned}$$

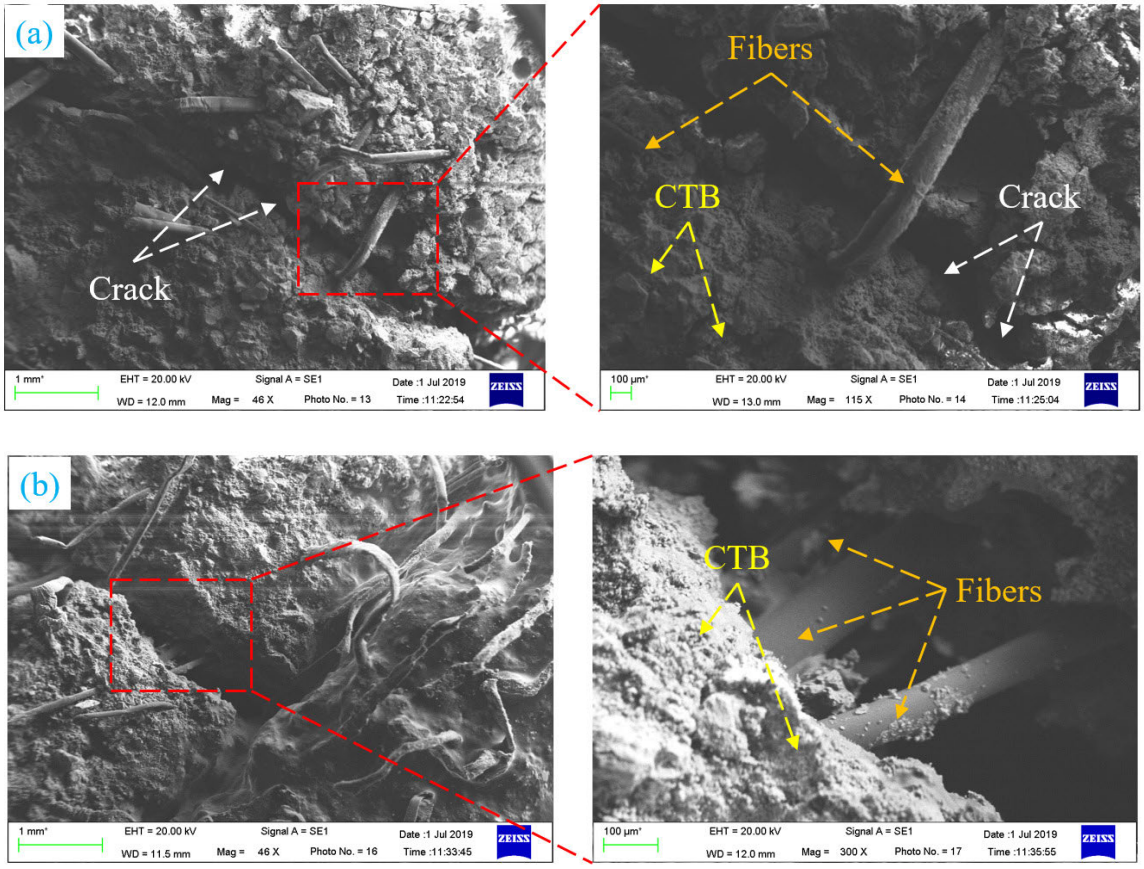

FIGURE 13. Typical optical and microstructural SEM images of fiber reinforced CTB samples.

where σ_1 and f_2 are normal and equal strengths (kPa). x_1, x_2, x_3 and x_4 denote FT, FC, SC and c/t, respectively.

As shown in FIGURE 11, the bending strength is the abscissa and the predicted value is ordinate. The dispersion of the coordinate points in this figure is small (close to the straight-line function y = x).

D. MICROSTRUCTURE OF FIBER REINFORCED CTB

FIGURE 12 shows a schematic view of fiber-reinforced mechanism on CTB sample under three-point bending loads. The surface microstructure mechanism of the CTB samples reinforced with fiber was scanned by means of the SEM test, as presented in FIGURE 13.

Taking one of CTB sample No. OE-14 as an example, it was found that fiber reinforced CTB specimen is subjected to tensile failure under a three-point bending load. Moreover, the internally doped fibers were completely exposed after the end of the bending experiment and fiber clusters showed a distinct stretched state. In other words, fibers are effectively prevented from deforming when CTB is deformed.

It is also found from FIGURE 13 that the fiber bridging effect between the cracks is very significant. Although CTB has cracked and deformed, fiber can effectively connect the block shaped CTB mix, so that fiber reinforced CTB samples undergoes large deformation, but there is no cause of instantaneous damage. Additionally, the shape of fiber has also been deformed, and it has changed from the original cylindrical to the flat column shape, indicating that the crack propagation drive fiber undergoes tensile deformation during the failure of CTB sample.

IV. CONCLUSION

In this study, a comprehensive laboratory work was carried out to better investigate the bending strength of fiber reinforced CTB samples. Orthogonal experiment are applied, and four kinds of FTs (polypropylene, polyacrylonitrile, glass and polyvinyl alcohol), FCs (0.2 wt.%, 0.4 wt.%, 0.6 wt.% and 0.8 wt.%), SCs (65 wt.%, 68 wt.%,70 wt.% and 75 wt.%) and c/ts (1:4, 1:6, 1:8 and 1:10) values are set in this study. The main conclusions of three-point bending strength test by fiber reinforced CTB samples are summarized as follows:

(1) The bending strength performance of CTB samples and the bearing capacity after the peak of the load-deflection curve were improved by adding fiber. The enhanced effect of polypropylene fiber was the best, and the optimum fiber content was 0.6 wt. %. With the increase of SC and c/t, the equivalent bending strength of fiber reinforced CTB samples increased gradually; the increase rate, however, decreased gradually.

(2) The order of the sensitivity of four factors on bending strength of fiber reinforced CTB is as follows: c/t > SC > FT > FC. The c/t and SC are still the main factors affecting bending strength. FT and FC are secondary factors, but the effect of fiber type is higher than that of fiber content.

(3) The deflection value of the samples entering the yield stage of fiber reinforced CTB samples was considerably larger than the peak deflection, and the equivalent bending strength of f_1 and f_2 after peak were mainly affected by the c/t and fiber content. In addition, the effect of the four factors on toughness of CTB samples after peak from large to small is in the order: FT, FC, c/t, and SC.

(4) The main influencing factor of the crack of fiber reinforced CTB was still the mechanical strength properties of CTB samples. The fiber cracking effect was mainly embodied in the crack propagation stage, and the fracture surface morphology was closely related to fiber properties and distribution quantity.

This research is part of a large research project studying behavior and properties of fiber reinforced cement-tailings matrix composites. It is clear from the executed results that bending strength of fiber reinforced samples has surpassed the commonly specified values. Hence, the results presented in this study are of vital importance and will be used as a baseline when establishing the final design of CTB samples. However, additional research should be performed to further improve bending strength and to advance fiber technology for in situ standards and applications.

ACKNOWLEDGMENT

The authors would also like to thank all staffs and technicians in the laboratory of the University of Science and Technology Beijing for their kind assistance during the performed tests. Special thanks are extended to two anonymous reviewers and editor for their constructive and helpful comments that significantly improved the overall quality of the revised manuscript.

REFERENCES

[1] M. Fall and O. Nasir, "Mechanical behaviour of the interface between cemented tailings backfill and retaining structures under shear loads," *Geotech. Geological Eng.*, vol. 28, pp. 779–790, Nov. 2010.
[2] E. Yilmaz, "Stope depth effect on field behaviour and performance of cemented paste backfills," *Int. J. Mining, Reclamation Environ.*, vol. 32, no. 4, pp. 273–296, 2018.
[3] Q.-S. Chen, Q.-L. Zhang, A. Fourie, X. Chen, and C.-C. Qi, "Experimental investigation on the strength characteristics of cement paste backfill in a similar stope model and its mechanism," *Construct. Building Mater.*, vol. 154, pp. 34–43, Nov. 2017.
[4] H. Lu, C. Qi, Q. Chen, D. Gan, Z. Xue, and Y. Hu, "A new procedure for recycling waste tailings as cemented paste backfill to underground stopes and open pits," *J. Cleaner Prod.*, vol. 188, pp. 601–612, Jul. 2018.
[5] D. Kump and T. Arnold, "Underhand cut-and-fill at the Barrick bullfrog mine," in *Underground Mining Methods: Engineering Fundamentals and International Case Studies*, W. Hustrulid and R. Bullock, Eds. Littleton, CO, USA: Society for Mining, Metallurgy and Exploration, 2001, ch. 69, pp. 345–350.
[6] L. Cui and M. Fall, "Multiphysics modeling of arching effects in fill mass," *Comput. Geotechnics*, vol. 83, pp. 114–131, Mar. 2017.
[7] S. Cao, W. Song, and E. Yilmaz, "Influence of structural factors on uniaxial compressive strength of cemented tailings backfill," *Construct. Building Mater.*, vol. 174, pp. 190–201, Jun. 2018.
[8] Q. Chen, Q. Zhang, C. Qi, A. Fourie, and C. Xiao, "Recycling phosphogypsum and construction demolition waste for cemented paste backfill and its environmental impact," *J. Cleaner Prod.*, vol. 186, pp. 418–429, Jun. 2018.
[9] E. Yilmaz, "Advances in reducing large volumes of environmentally harmful mine waste rocks and tailings," *Gospodarka Surowcami Mineralnymi*, vol. 27, no. 2, pp. 89–112, 2011.
[10] J. Wu, M. Feng, X. Mao, J. Xu, W. Zhang, X. Ni, and G. Han, "Particle size distribution of aggregate effects on mechanical and structural properties of cemented rockfill: Experiments and modeling," *Construct. Building Mater.*, vol. 193, pp. 295–311, Dec. 2018.
[11] A. Mousavi and E. Sellers, "Optimisation of production planning for an innovative hybrid underground mining method," *Resour. Policy*, vol. 62, pp. 184–192, Aug. 2019.
[12] S. Cao, E. Yilmaz, and W. Song, "Dynamic response of cement-tailings matrix composites under SHPB compression load," *Construct. Building Mater.*, vol. 186, pp. 892–903, Oct. 2018.
[13] A. Zrelli and T. Ezzedine, "Design of optical and wireless sensors for underground mining monitoring system," *Optik*, vol. 170, pp. 376–383, Oct. 2018.
[14] S. Cao, E. Yilmaz, W. Song, E. Yilmaz, and G. Xue, "Loading rate effect on uniaxial compressive strength behavior and acoustic emission properties of cemented tailings backfill," *Construct. Building Mater.*, vol. 213, pp. 313–324, 2019.
[15] Q. Sun, S. Tian, Q. Sun, B. Li, C. Cai, Y. Xia, X. Wei, and Q. Mu, "Preparation and microstructure of fly ash geopolymer paste backfill material," *J. Cleaner Prod.*, vol. 225, pp. 376–390, Jul. 2019.
[16] E. Yilmaz, T. Belem, and M. Benzaazoua, "Study of physico-chemical and mechanical characteristics of consolidated and unconsolidated cemented paste backfills," *Mineral Resour. Manage.*, vol. 29, no. 1, pp. 81–100, 2013.
[17] H. Jiang, H. Yi, E. Yilmaz, S. Liu, and J. Qiu, "Ultrasonic evaluation of strength properties of cemented paste backfill: Effects of mineral admixture and curing temperature," *Ultrasonics*, vol. 100, Jan. 2020, Art. no. 105983. doi: 10.1016/j.ultras.2019.105983.
[18] M. Fall and M. Pokharel, "Coupled effects of sulphate and temperature on the strength development of cemented tailings backfills: Portland cement-paste backfill," *Cement Concrete Compos.*, vol. 32, pp. 819–828, Nov. 2010.
[19] E. Yilmaz, T. Belem, and M. Benzaazoua, "One-dimensional consolidation parameters of cemented paste backfills," *Mineral Resour. Manage.*, vol. 28, no. 4, pp. 29–45, 2012.
[20] C. Qi, Q. Chen, A. Fourie, and Q. Zhang, "An intelligent modelling framework for mechanical properties of cemented paste backfill," *Minerals Eng.*, vol. 123, pp. 16–27, Jul. 2018.
[21] G. Xue, E. Yilmaz, W. Song, and S. Cao, "Compressive strength characteristics of cemented tailings backfill with alkali-activated slag," *Appl. Sci.*, vol. 8, no. 9, p. 1537, 2018.
[22] S. Cao and W. Song, "Medium-term strength and electromagnetic radiation characteristics of cemented tailings backfill under uniaxial compression," *Geotech. Geological Eng.*, vol. 36, pp. 3979–3986, Dec. 2018.
[23] W. Xu and P. Cao, "Fracture behaviour of cemented tailing backfill with pre-existing crack and thermal treatment under three-point bending loading: Experimental studies and particle flow code simulation," *Eng. Fract. Mech.*, vol. 195, pp. 129–141, May 2018.
[24] E. T. Asr, R. Kakaie, M. Ataei, and M. R. T. Mohammadi, "A review of studies on sustainable development in mining life cycle," *J. Cleaner Prod.*, vol. 229, pp. 213–231, Aug. 2019.
[25] J. Liu, W. Sui, and Q. Zhao, "Environmentally sustainable mining: A case study of intermittent cut-and-fill mining under sand aquifers," *Environ. Earth Sci.*, vol. 76, pp. 542–562, Aug. 2017.
[26] D. Kumar, U. K. Singh, and G. S. P. Singh, "Laboratory characterization of cemented rock fill for underhand cut and fill method of mining," *J. Inst. Eng. (India), Ser. D*, vol. 97, pp. 193–203, Oct. 2016.
[27] M. J. Raffaldi, J. B. Seymour, J. Richardson, E. Zahl, and M. Board, "Cemented paste backfill geomechanics at a narrow-vein underhand cut-and-fill mine," in *Rock Mechanics and Rock Engineering*. Vienna, Austria: Springer, 2019. doi: 10.1007/s00603-019-01850-4.
[28] L. Yang, E. Yilmaz, J. Li, H. Liu, and H. Jiang, "Effect of superplasticizer type and dosage on fluidity and strength behavior of cemented tailings backfill with different solid contents," *Construct. Building Materials.*, vol. 187, pp. 290–298, Oct. 2018.
[29] S. Cao, E. Yilmaz, and W. Song, "Evaluation of viscosity, strength and microstructural properties of cemented tailings backfill," *Minerals*, vol. 8, no. 8, p. 352, 2018.

[30] M. Benzaazoua, T. Belem, and E. Yilmaz, "Novel lab tool for paste backfill," *Can. Mining J.*, vol. 127, no. 3, pp. 31–32, 2006.
[31] E. Yilmaz, T. Belem, B. Bussière, and M. Benzaazoua, "Relationships between microstructural properties and compressive strength of consolidated and unconsolidated cemented paste backfills," *Cement Concrete Compos.*, vol. 33, pp. 702–715, Jul. 2011.
[32] H. Jiang, Z. Qi, E. Yilmaz, J. Han, J. Qiu, and C. Dong, "Effectiveness of alkali-activated slag as alternative binder on workability and early age compressive strength of cemented paste backfills," *Construct. Building Mater.*, vol. 218, pp. 689–700, Sep. 2019.
[33] E. Yilmaz, T. Belem, B. Bussière, M. Mbonimpa, and M. Benzaazoua, "Curing time effect on consolidation behaviour of cemented paste backfill containing different cement types and contents," *Construct. Building Mater.*, vol. 75, pp. 99–111, Jan. 2015.
[34] P. B. Hughes, R. Pakalnis, M. Hitch, and G. Corey, "Composite paste barricade performance at Goldcorp Inc. Red Lake Mine, Ontario, Canada," *Int. J. Mining, Reclamation Environ.*, vol. 24, pp. 138–150, 2010.
[35] B. Feng, X. Luo, J. Xu, and C. Weng, "Elimination of the adverse effect of cement filling on the flotation of a nickel ore," *Minerals Eng.*, vol. 69, pp. 13–14, Dec. 2014.
[36] M. Cai, "Prediction and prevention of rockburst in metal mines—A case study of Sanshandao gold mine," *J. Rock Mech. Geotech. Eng.*, vol. 8, pp. 204–211, Apr. 2016.
[37] G. Xue, E. Yilmaz, W. Song, and S. Cao, "Mechanical, flexural and microstructural properties of cement-tailings matrix composites: Effects of fiber type and dosage," *Compos. B, Eng.*, vol. 172, pp. 131–142, Sep. 2019.
[38] J. Sun, "Mechanics criterion and factors affecting overburden stability in solid dense filling mining," *Int. J. Mining Sci. Technol.*, vol. 27, pp. 407–413, May 2017.
[39] X. Du, G. Feng, Y. Zhang, Z. Wang, Y. Guo, and T. Qi, "Bearing mechanism and stability monitoring of cemented gangue-fly ash backfill column with stirrups in partial backfill engineering," *Eng. Struct.*, vol. 188, pp. 603–612, Jun. 2019.
[40] B. Yan, W. Zhu, C. Hou, and K. Guan, "A three-dimensional analytical solution to the arching effect in inclined backfilled stopes," *Geomech. Geoeng.*, vol. 14, no. 2, pp. 136–147, 2019.
[41] H. V. Le and D. J. Kim, "Effect of matrix cracking on electrical resistivity of high performance fiber reinforced cementitious composites in tension," *Construct. Building Mater.*, vol. 156, pp. 750–760, Dec. 2017.
[42] B. Akcay, "Experimental investigation on uniaxial tensile strength of hybrid fibre concrete," *Compos. B, Eng.*, vol. 43, pp. 766–778, Feb. 2012.
[43] M. Abdulkareem, J. Havukainen, and M. Horttanainen, "How environmentally sustainable are fibre reinforced alkali-activated concretes?" *J. Cleaner Prod.*, vol. 236, Nov. 2019, Art. no. 117601.
[44] A. Çavdar, "A study on the effects of high temperature on mechanical properties of fiber reinforced cementitious composites," *Compos. B, Eng.*, vol. 43, pp. 2452–2463, Jul. 2012.
[45] A. Lau and M. Anson, "Effect of high temperatures on high performance steel fibre reinforced concrete," *Cement Concrete Res.*, vol. 36, pp. 1698–1707, Sep. 2006.
[46] R. S. Olivito and F. A. Zuccarello, "An experimental study on the tensile strength of steel fiber reinforced concrete," *Compos. B, Eng.*, vol. 41, pp. 246–255, Apr. 2010.
[47] N. C. Consoli, H. P. Nierwinski, A. Peccin da Silva, and J. Sosnoski, "Durability and strength of fiber-reinforced compacted gold tailings-cement blends," *Geotextiles Geomembranes*, vol. 45, pp. 98–102, Apr. 2017.
[48] Z. H. Mohebi, A. B. Bahnamiri, and M. Dehestani, "Effect of polypropylene fibers on bond performance of reinforcing bars in high strength concrete," *Construct. Building Mater.*, vol. 215, pp. 401–409, Aug. 2019.
[49] K.-H. Yang, K.-H. Lee, J.-K. Song, and M.-H. Gong, "Properties and sustainability of alkali-activated slag foamed concrete," *J. Cleaner Prod.*, vol. 68, pp. 226–233, Apr. 2014.
[50] M. A. O. Mydin, N. A. Rozlan, and S. Ganesan, "Experimental study on the mechanical properties of coconut fibre reinforced lightweight foamed concrete," *J. Mater. Environ. Sci.*, vol. 6, no. 2, pp. 407–411, 2015.
[51] B. Roohollah, R. P. Hamid, A. H. Sadeghi, L. Masoud, and A. M. Ali, "Aninvestigation on adding polypropylene fibers to reinforce lightweight cement composites," *J. Eng. Fibres Fabrics.*, vol. 7, no. 4, pp. 13–21, 2012.
[52] K.-T. Lau, P.-Y. Hung, M.-H. Zhu, and D. Hui, "Properties of natural fibre composites for structural engineering applications," *Compos. B, Eng.*, vol. 136, pp. 222–233, Mar. 2018.
[53] R. J. Mitchell and D. M. Stone, "Stability of reinforced cemented backfills," *Can. Geotech. J.*, vol. 24, pp. 189–197, May 1987.
[54] X. W. Yi, G. W. Ma, and A. Fourie, "Compressive behaviour of fibre-reinforced cemented paste backfill," *Geotextiles Geomembranes*, vol. 43, pp. 207–215, Jun. 2015.
[55] X. Chen, X. Shi, J. Zhou, Q. Chen, E. Li, and X. Du, "Compressive behavior and microstructural properties of tailings polypropylene fibre-reinforced cemented paste backfill," *Construct. Building Mater.*, vol. 190, pp. 211–221, Nov. 2019.
[56] E. Galicia-Aldama, M. Mayorga, J. C. Arteaga-Arcos, and L. Romero-Salazar, "Rheological behaviour of cement paste added with natural fibres," *Constr. Building Mater.*, vol. 198, pp. 148–157, Feb. 2019.
[57] X. W. Yi, G. W. Ma, and A. Fourie, "Centrifuge model studies on the stability of fibre-reinforced cemented paste backfill stopes," *Geotextiles Geomembranes*, vol. 46, pp. 396–401, Aug. 2015.
[58] B.-W. Jo, S. Chakraborty, and Y. S. Lee, "Hydration study of the polymer modified jute fibre reinforced cement paste using analytical techniques," *Construct. Building Mater.*, vol. 101, pp. 166–173, Dec. 2015.
[59] M. Hambach and D. Volkmer, "Properties of 3D-printed fiber-reinforced Portland cement paste," *Cement Concrete Compos.*, vol. 79, pp. 62–70, May 2017.
[60] O. Onuaguluchi and N. Banthia, "Value-added reuse of scrap tire polymeric fibers in cement-based structural applications," *J. Cleaner Prod.*, vol. 231, pp. 543–555, Sep. 2019.
[61] G. Xue, E. Yilmaz, W. Song, and E. Yilmaz, "Influence of fiber reinforcement on mechanical behavior and microstructural properties of cemented tailings backfill," *Construct. Building Mater.*, vol. 213, pp. 275–285, Jul. 2019.
[62] G. Xue, E. Yilmaz, W. Song, and S. Cao, "Analysis of internal structure behavior of fiber reinforced cement-tailings matrix composites through X-ray computed tomography," *Compos. B, Eng.*, vol. 175, Oct. 2019, Art. no. 107091.
[63] K. C. Kim, I. H. Yang, and C. B. Joh, "Effects of single and hybrid steel fiber lengths and fiber contents on the mechanical properties of high-strength fiber-reinforced concrete," *Adv. Civil Eng.*, vol. 2018, Feb. 2018, Art. no. 7826156.
[64] S. Cao, E. Yilmaz, and W. Song, "Fiber type effect on strength, toughness and microstructure of early age cemented tailings backfill," *Constr. Building Material.*, vol. 223, pp. 44–54, Oct. 2019.
[65] G. Araya-Letelier, J. Concha-Riedel, F. C. Antico, C. Valdés, and G. Cáceres, "Influence of natural fiber dosage and length on adobe mixes damage-mechanical behavior," *Construct. Building Mater.*, vol. 174, pp. 645–655, Jun. 2018.
[66] M. K. Hagnell and M. Åkermo, "The economic and mechanical potential of closed loop material usage and recycling of fibre-reinforced composite materials," *J. Cleaner Prod.*, vol. 223, pp. 957–968, Jun. 2019.
[67] B. Koohestani, A. K. Darban, P. Mokhtari, E. Yilmaz, and E. Darezereshki, "Comparison of different natural fiber treatments: A literature review," *Int. J. Environ. Sci. Technol.*, vol. 16, pp. 629–642, Jan. 2019.
[68] H. Awang, M. A. O. Mydin, and A. F. Roslan, "Effects of fibre on drying shrinkage, compressive and flexural strength of lightweight foamed concrete," *Adv. Mater. Res*, vol. 587, pp. 144–149, Nov. 2012.
[69] K. Zhang, L. Pan, J. Li, C. Lin, Y. Cao, N. Xu, and S. Pang, "How does adsorption behavior of polycarboxylate superplasticizer effect rheology and flowability of cement paste with polypropylene fiber?" *Cement Concrete Compos.*, vol. 95, pp. 228–236, Jan. 2019.
[70] D. A. Landriault, "Backfill in underground mining," in *Underground Mining Methods: Engineering Fundamentals and International Case Studies*, W. Hustrulid and R. L. Bullock, Eds. Littleton, CO, USA: Society for Mining, Metallurgy and Exploration, ch. 69, 2001, pp. 601–614.
[71] D. F. McCarthy, *Essentials of Soil Mechanics and Foundations: Basic Geotechnics*, 7th ed. London, U.K.: Pearson, 2017, pp. 1–864.
[72] H. Li, A. Wu, and H. Wang, "Evaluation of short-term strength development of cemented backfill with varying sulphide contents and the use of additives," *J. Environ. Manage.*, vol. 239, pp. 279–286, Jun. 2019.
[73] E. Yilmaz and M. Guresci, "Design and characterization of underground paste backfill," in *Paste Tailings Management*, E. Yilmaz and M. Fall, Eds. New York, NY, USA: Springer, 2017, ch. 5, pp. 1–36. doi: 10.1007/978-3-319-39682-8_5.
[74] Y. Zhao, J. Gao, F. Chen, C. Liu, and X. Chen, "Utilization of waste clay bricks as coarse and fine aggregates for the preparation of lightweight aggregate concrete," *J. Cleaner Prod.*, vol. 201, pp. 706–715, Nov. 2018.
[75] *Standard test methods for fiber reinforced concrete structures. China Association for Engineering Construction Standardization*, Tech. Committee Standards Concrete Struct., Beijing, China, 2009, vol. 13.

SHUAI CAO received the B.S., M.S., and Ph.D. degrees in mining engineering from the University of Science and Technology Beijing, China, where he currently holds a postdoctoral position with the School of Civil and Resources Engineering. He has published nearly 20 high-quality journals. His research interests include underground mining methods and fiber-reinforced cemented tailings backfill. He has served as a Reviewer for over ten journals.

GAILI XUE received the B.S. degree in mining engineering from the University of Science and Technology Liaoning, Anshan, China, and the M.S. degree in mining engineering from the University of Science and Technology Beijing (USTB), China, where she is currently pursuing the Ph.D. degree. She has published nearly six high-quality journals. Her research interests include fiber-reinforced cemented tailings backfill, and rock and soil mechanics.

EROL YILMAZ was born in Rize, Turkey. He received the B.Sc. degree (Hons.) in mining engineering from the University of Istanbul, in 2000, the M.Sc. degree in mining engineering from Karadeniz Technical University, Trabzon, Turkey, in 2003, and the Ph.D. degree in environmental sciences from UQAT, Rouyn-Noranda, QC, Canada, with a focus on hydro-mechanical and geotechnical properties of cemented paste backfill. From July 2000 to July 2004, he was an Expert with the Department of Mining Engineering, Karadeniz Technical University. In August 2004, he moved to Canada to work in an international project at the URSTM Lab of the University of Quebec at Abitibi-Temiscamingue UQAT. He was also a Postdoctoral Fellow at UQAT, focusing on physical and geochemical behavior of surface paste disposal at Agnico Eagle's LaRonde Mine, Cadillac, QC. He is currently with Cayeli Copper-Zinc Mine, First Quantum Minerals Ltd., Rize, as a Paste Backfill and Batch Plant Engineer. He has more than 15 years of rich experience in industry, academia, and research by focusing on mine tailings, paste systems, cemented paste backfill, surface paste disposal, underground mine backfill, mine wastes management, environmental geomechanics, rock mechanics, mining engineering, and mineral processing. He authored or coauthored many scientific publications, such as books, reports, and journal and conference articles. He has been a member of the Canadian Institute of Mining, Metallurgy and Petroleum and the Turkish Institute of Mining Engineers, since 2005 and 2000, respectively. He has been repeatedly invited as a Keynote Speaker or a Lecturer and regularly acts as a Consultant and a Reviewer for several scientific committees, peer-reviewed journals, funding agencies, and several international projects.